

First-principles calculations of the adsorption, diffusion, and dissociation of a CO molecule on the Fe(100) surface

Dan C. Sorescu,¹ Donald L. Thompson,² Margaret M. Hurley,³ and Cary F. Chabalowski⁴

¹*U.S. Department of Energy, National Energy Technology Laboratory, P.O. Box 10940, Pittsburgh, Pennsylvania 15236 and Department of Chemical and Petroleum Engineering, University of Pittsburgh, Pittsburgh, Pennsylvania 15261*

²*Department of Chemistry, Oklahoma State University, Stillwater, Oklahoma 74078*

³*U.S. Army Research Laboratory, AMSRL-CI-HA, Aberdeen Proving Ground, Maryland 21005-5067*

⁴*U.S. Army Research Laboratory, AMSRL-WM-BD, Aberdeen Proving Ground, Maryland 21005-5066*

(Received 19 November 2001; published 25 July 2002)

First-principles pseudopotential plane wave calculations based on spin-polarized density functional theory (DFT) and the generalized gradient approximation (GGA) have been used to study the adsorption of CO molecules on the Fe(100) surface. Among several possible adsorption configurations considered here, the most stable corresponds to a fourfold state in which a CO molecule is tilted relative to the surface normal by 50°. In this case, the CO bond is elongated to 1.32 Å and has a low vibrational stretching frequency of 1246 cm⁻¹ to be compared with the experimental gas phase value of 2143 cm⁻¹. The adsorption energy for this state is found to vary between 46.7 and 43.8 kcal/mol depending on the choice of exchange-correlation functional used in the DFT. A total of three adsorption sites have been located, and the relative adsorption energies are $E(\text{fourfold}) > E(\text{twofold}) \approx E(\text{onefold})$ at lower surface coverage, and $E(\text{fourfold}) > E(\text{onefold}) > E(\text{twofold})$ at higher coverage. A similar analysis performed for the C and O atoms indicates that the adsorption at the fourfold site is the most stable among various configurations, with adsorption energies of 186 and 145 kcal/mol, respectively. Additionally, we have demonstrated the possibility that a C atom embeds into the lattice in a twofold, bridgelike configuration with an adsorption energy of 154 kcal/mol. The minimum energy pathways for the surface diffusion of a CO molecule between selected pairs of local minima indicate that the barriers for these processes are generally quite small with values less than 2 kcal/mol. One exception to this is the diffusion out of the most stable fourfold site, where the barrier is predicted to be around 13 kcal/mol. Finally, the barriers for dissociation of CO bound in a fourfold site have been calculated to have values in the range of 24.5–28.2 kcal/mol, supporting the experimental observation that dissociation of CO bound to the surface seems to compete with CO desorption at 440 K.

DOI: 10.1103/PhysRevB.66.035416

PACS number(s): 68.43.Hn, 31.15.Ew, 82.37.Np

I. INTRODUCTION

Understanding the interaction of carbon monoxide with transition-metal surfaces, and in particular with iron surfaces, is of primary importance as this system can be involved in many catalytic processes such as oxidation, methanation, or Fischer-Tropsch synthesis of aliphatic hydrocarbons.^{1–3} Additionally, CO has been identified as one of the products of incomplete combustion of propellants in gun tubes with important contributions to the erosion process of these materials. This is not surprising, since it has long been known that iron (the primary component of steel) acts as a catalyst in the Boudard and Fischer-Tropsch reactions,⁴ both of which deposit carbon into the surface of iron to form steel. In addition to industrial applications, CO can also be used as a probe adsorbate to provide fundamental information about gas-surface interactions, the adsorption sites, and chemical reactions on different surfaces.⁵ Therefore, there is significant industrial and fundamental scientific motivation to understand various elementary processes such as chemisorption, diffusion, and dissociation of CO molecules on Fe surfaces.

The interaction of a CO molecule with a Fe(100) surface has been the subject of previous experimental studies,^{6–13} which indicated the existence of a rich chemistry for this system. Based on x-ray photoelectron spectroscopy (XPS)

and temperature programmed desorption (TPD) measurements, Moon *et al.*⁶ observed that CO adsorbs molecularly at low temperatures and dissociates above 440 K. The dissociated atomic species C and O recombine and desorb as CO molecules around 800 K. The adsorption process was associated with filling sequentially three states corresponding to three types of binding configurations of CO molecules on the surface. It has been shown that the most tightly bound molecular state, denoted CO(α_3), is the precursor to dissociation of CO at 440 K.^{6a} The other two molecular states CO(α_2) and CO(α_1) desorb molecularly below 300 K without dissociation.⁷ Based on the assumption of a simple first-order desorption process with a preexponential factor of 10¹³ s⁻¹, the activation energies for desorption from the three states $\alpha_3, \alpha_2, \alpha_1$ were estimated to be 26.2, 18.0, and 12.8 kcal/mol, respectively.^{6a} Later experiments^{6b} suggested that a pre-exponential factor of 10¹³ s⁻¹ might be too small for these types of systems, and a better estimate would be somewhere in the range 10¹⁵ to 10¹⁸ s⁻¹. Based on a simple rate constant expression such as $k = A \exp(-E/RT)$ where E is the activation energy (taken here to be the heat of desorption), T the experimentally observed desorption temperatures (440, 306, and 220 K for $\alpha_3, \alpha_2,$ and α_1 states, respectively),^{6a} R the gas constant, and A the pre-exponential factor set equal to either 10¹⁵ or 10¹⁸ s⁻¹, the adjusted ex-

perimental activation energies for desorption from the α_3 , α_2 , α_1 states would be 32–36, 22–25, and 16–18 kcal/mol, respectively.

The molecular structure corresponding to the binding state CO(α_3) has been further characterized by both near edge x-ray absorption fine structure (NEXAFS) (Ref. 8) and high resolution electron energy loss spectroscopy (HREELS).⁹ It was determined that in this state the molecule adsorbs at the fourfold hollow site in a tilted configuration relative to the surface normal at an angle between $45^\circ \pm 10^\circ$ and $55^\circ \pm 2^\circ$.¹⁰ Such a binding configuration allows for an increase of the interaction between the O atom of the CO molecule and the iron surface atoms. As a result of the increased interaction with the surface, the C-O bond is elongated by an estimated value of $0.07 \pm 0.02 \text{ \AA}$ relative to the bonds of the other molecularly adsorbed CO(α_2) and CO(α_1) species.⁸ The elongated C-O bond in the tilted configuration presents an extremely low stretching frequency of 1210 cm^{-1} to be compared with the isolated CO molecule (2143 cm^{-1}).⁹ This suggests a significant weakening of the CO bond and a change in the bonding character from a triple-bond for the isolated molecule to a single-bond character in the α_3 state. In contrast, the vibrational frequencies of the other two states α_2 and α_1 , are reported to be much higher with values of 2020 and 2070 cm^{-1} , respectively.⁷ The precise structural assignments of these states were not made, but it was suggested based on the vibrational frequency analysis that the α_2 state corresponds to a twofold bridged configuration while the α_1 state has CO bound in a onefold site on top of a single Fe atom.⁷ The nomenclature onefold, twofold, and fourfold derives from the number of nearest-neighbor iron atoms in close contact with the carbon in CO. Further insight into the chemical character of the three bonding states has been provided based on ultraviolet photoelectron spectroscopy (UPS) measurements.¹¹ It was determined that in the α_3 state there is extensive rehybridization of the orbitals within the molecule, while in the other two states α_2 and α_1 , the valence band data correspond to a typical chemisorbed CO.

Direct information about the mechanism of CO dissociation at low exposures was provided by HREELS studies.^{12,13} It was observed that the CO stretching frequency for the α_3 state increases with coverage, and decreases with temperature.¹² At an exposure of 0.1 L, increasing the temperature from 103 to 373 K was accompanied by an increase in the intensity of the vibrational Fe-C and Fe-O peaks with a simultaneous decrease in the C-O stretching intensity and frequency, which dropped from 1170 to 1150 cm^{-1} . Based on these findings it was argued that there is clear evidence that the CO molecule adsorbed in the α_3 state represents the precursor for dissociation on the Fe(100) surface.

In contrast to the relatively large number of experimental techniques used to investigate various aspects of the adsorption and dissociation processes of CO on iron surfaces, there are few theoretical studies focused on this subject.^{14–18} Among these, the earlier theoretical work was based on the use of either semiempirical methods or low level Hartree-Fock *ab initio* calculations performed on various small clusters.^{14–16} More recently, different aspects of the CO ad-

sorption on the Fe(100) surface have been analyzed using first principles density functional theory (DFT) calculations.^{17,18} However, some large discrepancies can be seen when comparing the results provided by these two studies.^{17,18} Aray and Rodriguez¹⁷ employed DFT plane wave calculations to predict that “CO adsorption on the fourfold site is 67.566 kcal/mol more stable than the bridging site, whereas this latter is 16.193 kcal/mol more stable than the onefold site.” These calculated values are significantly different from the experimental activation energies of 26.2, 18.0, and 12.8 kcal/mol determined in Ref. 6a for the adsorption states α_3 , α_2 and α_1 , respectively. On the other hand, Nayak, Nooijen, Bernasek, and Blaha (NNBB),¹⁸ using DFT methods applied to a cluster model, have determined binding energies for CO of 37.4 kcal/mol for the adsorption on the fourfold hollow site, 32.3 kcal/mol for the on-top position and 24.7 kcal/mol for the twofold site. These last values are clearly closer to the range of experimental data⁶ but differ significantly from the results reported by Aray and Rodriguez.¹⁷

In an attempt to clarify the adsorption properties of CO on the Fe(100) surface, we report here the results of first-principles density functional theory calculations within the pseudopotential approximation. The periodic nature of the surface, which is essentially neglected in simple cluster models, has been considered in the present case by the aid of a slab model (supercell model) repeated periodically in all three dimensions. The role of lateral CO···CO interactions (modeling percent surface coverage) on the adsorption process has been considered also. In addition to molecular CO interactions with the Fe(100) surface, we report the adsorption properties of individual C and O atoms on the surface. Furthermore, the effect of lattice strain on the chemisorption energies of CO, C, and O species has been investigated. We analyze also selected minimum energy pathways for diffusion of a CO molecule between different adsorption sites, as well as for the dissociation of a CO molecule adsorbed at the fourfold hollow site.

Throughout the paper the terms “onefold” and “on-top” configuration will be used interchangeably, as will be “two-fold” and “bridged” configuration. The organization of the paper is as follows. In Sec. II we describe the computational methods used in the present study. The results of total energy calculations for adsorption of CO, C, and O species as well as for the diffusion and dissociation paths are given in Sec. III. Finally, we summarize the main conclusions in Sec. IV.

II. COMPUTATIONAL METHOD

The calculations performed in this study were done using the *ab initio* total-energy and molecular dynamics program VASP (Vienna *ab initio* simulation program) and the ultrasoft pseudopotential database contained therein.^{19–21} This program evaluates the total energy of periodically repeating geometries based on density-functional theory and the pseudopotential approximation. In this case the electron-ion interaction is described by fully nonlocal optimized ultrasoft pseudopotentials (USPP’s) similar to those introduced by Vanderbilt.^{22,23} The USPP’s include nonlinear core correc-

tions to account for possible valence-core charge interactions due to the $3d$ valence states overlapping with the $3p$ semi-core states in iron.²⁴ Periodic boundary conditions are used, with the one electron pseudoorbitals expanded over a plane wave basis set. The expansion includes all plane waves whose kinetic energy is less than a predetermined cutoff energy E_{cut} , i.e., $\hbar^2 G_{\text{cut}}^2/2m < E_{\text{cut}}$, where $G_{\text{cut}} > |k + G|$, and G is the reciprocal lattice vector, m the electronic mass, and k is one of the k points used to sample the Brillouin zone. The k points are obtained from the Monkhorst-Pack scheme.²⁵

Electron smearing is employed via the Methfessel-Paxton technique,²⁶ with a smearing width consistent with $\sigma = 0.1$ eV, in order to minimize the errors in the Hellmann-Feynman forces due to the entropic contribution to the electronic free energy.^{20,21} All energies are extrapolated to $T = 0$ K. The minimization of the electronic free energy is carried out using an efficient iterative matrix-diagonalization routine based on a sequential band-by-band residuum minimization method (RMM),^{20,21} or alternatively, based on preconditioned band-by-band conjugate-gradient (CG) minimization.²⁷ The optimization of different atomic configurations is based upon a conjugate-gradient minimization of the total energy. The value of E_{cut} and the k -point grid are chosen to ensure the convergence of energies and structures.

The minimum energy paths between different minima were optimized by use of the nudged elastic band (NEB) method of Jónsson and co-workers.²⁸ In this approach, the reaction path is “discretized,” with the discrete configurations, or images, between minima being connected by elastic springs to prevent the images from sliding to the minima in the optimization. In the NEB searches, either 8 or 16 images were employed between minima.

Unless otherwise stated, the calculations have been done using the spin polarized PW91 generalized gradient approximation (GGA) of Perdew *et al.*²⁹ The effect of using a different exchange-correlation functional on the adsorption energies has been investigated by using the revised form of the Perdew, Burke, and Ernzerhof (PBE)³⁰ functional as introduced by Hammer *et al.*³¹ (revPBE) and implemented in the commercial version of the software package CASTEP (Cambridge serial total energy package).³² Once again USPP’s have been used, and electron smearing is done according to a gaussian distribution with a minimum smearing width parameter of $\sigma = 0.1$ eV.

To determine the degree of convergence with respect to E_{cut} and the number of k points, a series of calculations have been performed on bulk iron, the bare surface, the isolated CO molecule, and CO bound to the surface. Prior to any geometry optimizations, iron is assumed to be in its body-centered cubic (bcc) lattice. Testing various k -point grids shows the cell parameters and bulk modulus for bulk iron to be converged to less than 1% at a grid of $11 \times 11 \times 11$ (consisting of 56 total k points in the irreducible Brillouin zone). With this grid, values for E_{cut} at or above 300 eV produce an absolute error in the total energy of less than 1 meV/atom, in agreement with previous DFT results obtained by Moroni *et al.*²⁴ The total energy and bond length for the isolated CO molecule have been tested at several E_{cut} values. These prop-

erties are found to change by only 0.0024 eV (0.06 kcal/mol) and 0.004 Å (0.03%) in going from $E_{\text{cut}} = 495$ to 595 eV. This is sufficiently converged for the purposes of this study. To ensure a consistent set of convergence criteria for systems containing the CO molecule, a cutoff energy of 495 eV has been used for all the VASP calculations (including the bulk and bare Fe slab systems). All surface calculations that include CO, C, or O are done using a supercell consisting of 2×2 unit cells in the plane of the slab, with a vacuum distance of 10 Å. Finally, for CO bound to the fourfold site, changing the k -point grids from $4 \times 4 \times 2$ to $6 \times 6 \times 2$ gave a change in the total energy of less than 0.007 eV, and a change in the CO bond length and the Fe-O nearest-neighbor distances of less than 0.1%. Therefore, a grid of $4 \times 4 \times 2$ is used in all surface calculations unless otherwise stated.

III. RESULTS AND DISCUSSIONS

A. Calculations for bulk Fe

A number of tests have been performed to benchmark the accuracy of the method when applied to bulk iron, the bare surface, and isolated CO. In order to determine the equilibrium bulk parameters of Fe, we have uniformly scaled the lattice vectors and calculated the energy as function of the unit cell volume. The data were then fit with the Murnaghan equation of state,³³ which predicted a lattice constant of 2.8653 Å and a bulk modulus of $B_0 = 1.597$ Mbar. These values differ by -0.16 and -4.94 % from the corresponding experimental values of 2.87 Å and 1.68 Mbar, respectively.³⁴ At the optimized structure, the magnetic moment per atom for this ferromagnetic bcc phase of Fe is found to be $2.33 \mu_B$, in good agreement with the experimental value of $2.22 \mu_B$ (Ref. 34) and previous DFT results ($2.32 \mu_B$).^{24,35} The corresponding saturation magnetization is 1844.4 Gs, which is about 5.3% larger than the experimental value of 1750 Gs.³⁴ These values indicate that the present set of pseudopotentials, as well as the k -point density and the cutoff energy E_K , are able to provide a very good representation of the structural properties of bulk Fe with only slightly larger discrepancies for the magnetic properties.

B. Slab calculations for the Fe(100) surface

In the case of the Fe(100) surface, Wang *et al.*³⁶ have determined from low-energy electron diffraction (LEED) studies that small relaxations of about 0.07 Å exist in the top two layers of the Fe(100) surface. The spacing between the top two layers (Δd_{1-2}) decreases by -5 ± 2 % relative to the bulk interlayer spacing, and the distance between the next two layers (Δd_{2-3}) increases by 5 ± 2 % relative to the bulk. The problem of surface relaxation is studied by relaxing the top two layers of iron atoms while freezing the coordinates of the remaining atoms at their bulk optimized positions. This has been done as a function of the number of iron layers in the slab, and the results are presented in Table I. As indicated in this table, when the number of layers in the slab is increased above four layers the interlayer separation oscillates around the average values of -4.0 % for Δd_{1-2} and 2.7 % for Δd_{2-3} . Contraction between the top two layers,

TABLE I. Percent change in the layer separations relative to the bulk value “ d ” as a result of atomic relaxation of the top two layers and as a function of the number of layers in the slab.

	4 L	5 L	6 L	7 L	8 L	10 L	12 L	Exp. ^a
$\Delta d_{1-2}/d$	-2.7	-4.3	-2.6	-3.8	-4.2	-4.0	-3.9	$-5.0 \pm 2\%$
$\Delta d_{2-3}/d$	4.0	3.1	3.1	2.7	2.7	3.0	2.7	$5.0 \pm 2\%$

^aReference 36.

and expansion between the next two layers are consistent with experiment. In addition, these types of relaxations are similar to those obtained by NNBB (Ref. 18) based on FLAPW periodic slab calculations, where they reported relaxations of -4% for Δd_{1-2} and 1.5% for Δd_{2-3} . It is interesting to note that Mortensen *et al.*³⁵ using similar DFT plane-wave calculations for Fe(100) surface have determined relaxations for Δd_{1-2} of -1% , and Δd_{2-3} of 5% using a four layer model with the top two layers relaxed. As seen from the data in Table I our results for the case of the four-layer system differ the most from those obtained using a larger number of layers. This fact indicates that such a slab might not be sufficiently large to provide an accurate description of the relaxations seen experimentally. Consequently, slabs containing six layers are used throughout this study with one exception. This corresponds to a check on the adequacy of the six layer slab by comparing the corresponding adsorption properties of CO to those obtained for a seven layer slab. These results will be discussed in the appropriate section.

C. Test calculations for the isolated CO molecule

The optimization of the isolated CO molecule in a large cubic box of $10 \times 10 \times 10 \text{ \AA}^3$ predicts an equilibrium CO bond length of 1.145 \AA , which differs by only 1.5% from the experimental value of 1.128 \AA .³⁷ Similarly good agreement is obtained with experiment for the vibrational C-O stretching frequency, where the calculated value is 2174 cm^{-1} and the experimental value is 2143 cm^{-1} .³⁷ Finally we have evaluated the atomization energy for the CO molecule using the individual energies of CO, C, and O species as well as the corresponding zero point energy for CO. Our calculated value of 259.7 kcal/mol is in very good agreement with experimental data (259.2 kcal/mol) (Ref. 37) and practically coincides with the previous result reported by Hammer *et al.*³¹ using the PW91 functional. The good agreement of our results for bulk Fe, the bare surface, and for the isolated molecule with data obtained in other theoretical or experimental studies allows us to proceed with confidence to the main focus of this study, i.e., the investigation of CO adsorption on the Fe(100) surface.

D. CO adsorption on the Fe(100) surface

Unless otherwise stated, the calculations for the adsorption of a CO molecule on the Fe(100) surface have been done using a 2×2 slab with six layers containing a total of 24 Fe atoms. In a limited number of instances we have used, for testing purposes, a slab with seven layers containing 28 Fe atoms. In all cases the relaxation of the CO molecule has been done together with the Fe atoms in the first two layers

of the slab. The remaining atoms of the slab have been frozen at the bulk optimized positions. The dependence of the adsorption energies on the percent of CO surface coverage has been analyzed by considering one or two CO molecules in the supercell, such that each supercell is then defined as having a fractional coverage of either $\theta=0.25$ or $\theta=0.5$, respectively. The main adsorption sites and molecular configurations considered in this study are depicted in Fig. 1. Table II contains all the geometrical and energetic data describing the CO adsorbed on the surface. For the case of a tilted CO, the tilt angle is defined as the angle formed by the CO bond and a vector drawn normal to the surface. The vibrational frequency is given in the column labeled by “ ν ,” and the energy of adsorption to the surface by an atom or molecule is given in the column labeled “ E_{ads} ” in units of kcal/mol. All other entries are defined in the footnotes to the table.

For all configurations, the corresponding adsorption energies are calculated according to the expression

$$E_{\text{ads}} = E_{\text{CO}} + E_{\text{slab}} - E_{(\text{CO}+\text{slab})}, \quad (1)$$

where E_{CO} is the energy of the isolated CO molecule in equilibrium position, E_{slab} is the total energy of the relaxed slab, and $E_{(\text{CO}+\text{slab})}$ is the total energy of the optimized adsorbate/slab system (including relaxation of the top two Fe layers). A positive E_{ads} corresponds to a stable adsorbate/slab

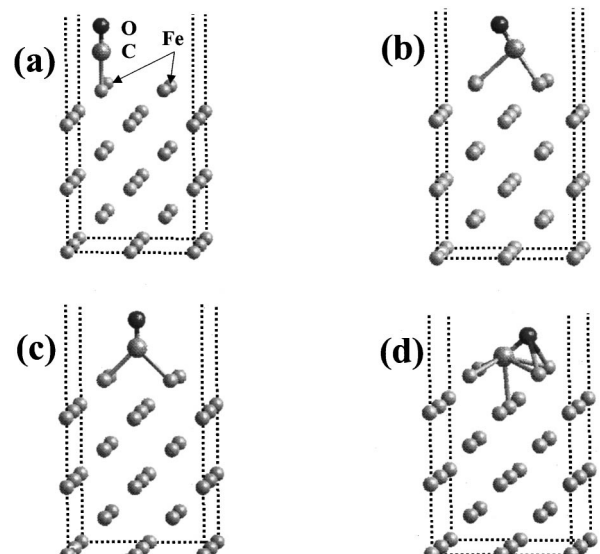


FIG. 1. The adsorption configurations of CO on the Fe(100) surface. (a) Onfold (on-top) configuration; (b) twofold tilted (bridged) configuration; (c) twofold vertical configuration; (d) fourfold hollow site configuration.

TABLE II. Calculated equilibrium distances and adsorption energies for the CO molecule adsorbed on the Fe(100) surface at different sites and for different coverages θ . Results from experiment and other theoretical studies are included for comparison.

Configuration	θ	$r(\text{C-O})$ (Å)	$r(\text{Fe-C})^a$ (Å)	$r(\text{Fe-O})^a$ (Å)	$h(\text{C-surf})^b$ (Å)	φ^c (deg.)	ν (cm^{-1})	E_{ads} (kcal/mol)
Present work, PW91 functional (six layers slab model)								
CO (isolated)		1.1453					2174	
onifold	0.25	1.177	1.782	2.959	1.777	0.0	1887	34.1
	0.50	1.172	1.811	2.983	1.811	0.0		33.4
twofold tilt	0.25	1.193	1.807	2.717	1.497	31.7	1784	34.8
	0.50	1.186	1.861	2.775	1.432	25.0		30.9
twofold vert.	0.25	1.196	1.957	2.923	1.370	0.0		32.9
	0.50	1.189	1.973	2.928	1.372	0.0		26.0
fourfold	0.25	1.322	1.970	2.124	0.65/0.58	50.2	1246	46.7
	0.50	1.319	1.992	2.118	0.58/0.57	50.1		48.1
fourfold vert.	0.25	1.255	2.140	2.810	0.69	0.0		36.7
Present work, RPBE functional (six layers slab model)								
CO (isolated)		1.1439					2169	
onifold	0.25	1.178	1.779	2.957	1.779	0.0		32.1
twofold tilt	0.25	1.188	1.801	2.769	1.505	29.4		32.3
twofold vert.	0.25	1.196	1.959	2.923	1.136	0.0		29.7
fourfold	0.25	1.316	1.966	2.128	0.63/0.56	48.0		43.8
Present work, PW91 functional (seven layers slab model)								
onifold	0.25	1.176	1.779	2.955	1.779	0.0		32.1
twofold tilt	0.25	1.193	1.806	2.723	1.147	28.7		34.4
twofold vert.	0.25	1.198	1.950	2.913	1.135	0.0		32.8
fourfold	0.25	1.321	1.968	2.134	0.64/0.57	49.0		46.9
Reference 18, cluster model (DFT)								
onifold		1.19	1.82	3.01		0.0	1888	32.3
twofold vert.		1.21	2.12	3.11		0.0	1693	24.7
fourfold		1.32	1.90	2.23		54.0		37.4
Reference 18, slab model (FLAPW)								
onifold		1.17	1.82	3.00		0.0		
twofold vert.		1.18	1.95	2.91		0.0		
fourfold		1.30	1.98	2.10		54.0		
Exp.								
CO (isolated) ^d		1.1283					2143	
onifold							2070 ^e	12.8 ^g
twofold							2020 ^e	18.0 ^g
fourfold						45.0 ± 10^h 55.0 ± 2^i	1210 ^e	$26.2,^g 37.0^f$

^aFor the two fold tilted and four fold configurations the Fe-C or Fe-O represents the shortest distances to the Fe atoms involved in binding.

^b h represents the height of the C atom in CO above the surface. In the four fold site, the two distances refer to the average for pairs of Fe atoms in the first layer considered nonbonded and bonded to the O atom, respectively.

^c φ represents the angle between the C-O and the normal to the surface.

^dReference 37.

^eReferences 7 and 9.

^fReference 39.

^gReference 6a.

^hReference 8.

ⁱReference 10.

system. It is assumed that the adsorption process has no barrier, thus allowing for the comparison of the experimental desorption activation energies with the calculated adsorption energies. The energy of the isolated CO molecule for this

calculation is that of the optimized molecule as described in a previous section. The same Brillouin-zone sampling has been used to calculate the properties of the bare slab and of the adsorbate-slab systems. The resulting geometric and en-

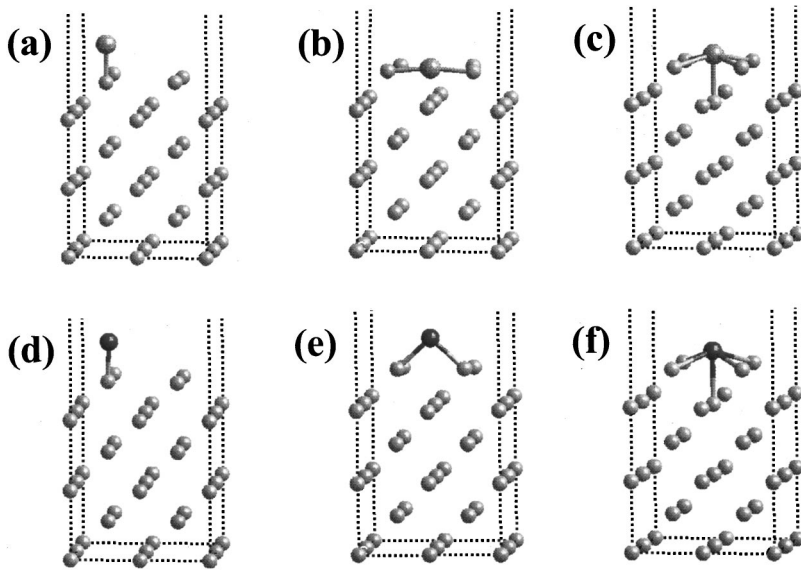


FIG. 2. The adsorption configurations of individual C and O atoms on the Fe(100) surface: (a) and (d) onefold configurations; (b) and (e) are twofold bridged configurations; (c) and (f) fourfold configurations.

ergetic parameters for various binding configurations of CO on the Fe(100) surface are given in Table II, while the molecular configurations are represented in Fig. 1.

Onefold (on-top) site. In this configuration CO adsorbs perpendicular to the surface with the carbon down, and situated directly above a surface Fe atom [see Fig. 1(a)] at an interatomic distance of $R(\text{Fe-C}) = 1.177 \text{ \AA}$. For this configuration the CO bond is slightly elongated by 0.032 \AA relative to the isolated gas phase equilibrium distance, with an adsorption energy of 34.1 kcal/mol at $\theta = 0.25$. We have also analyzed the $\theta = 0.5$ case where two CO molecules are arranged in a next-nearest-neighbor configuration. For this case there is a small decrease in the adsorption energy to 33.4 kcal/mol presumably due to lateral $\text{CO} \cdots \text{CO}$ repulsive interactions.

Previous work from Nørskov's group³¹ has indicated that using the revised form of the PBE (revPBE) functional proposed by Zhang and Yang³⁸ improves the agreement with experimental data for the calculated chemisorption energies of atoms and molecules on transition-metal surfaces. We

TABLE III. Calculated equilibrium distances and adsorption energies for C and O atoms adsorbed on the Fe(100) surface at different sites for a coverage $\theta = 0.25$. The results have been obtained using the PW91 functional.

Configuration	$r(\text{Fe-X})$ (\AA)	$r(\text{X-surf})$ (\AA)	E_{ads} (kcal/mol)
C atom			
one fold	1.605	1.605	118.0
two fold	1.735	0.127 ^a	154.0
four fold	1.967	0.396	186.0
O atom			
one fold	1.642	1.642	111.0
two fold	1.833	1.241	132.0
four fold	2.095	0.613	145.0

^aC atom embeds into the lattice, forming an angle with surface atoms Fe-C-Fe of 171.5° .

have tested this point for $\theta = 0.25$ using the revPBE functional including reoptimization of the internal geometrical parameters of the CO molecule as well as its position and orientation relative to the surface. In these calculations the Fe surface has been kept frozen at the optimized structure for a bound CO determined from the PW91 functional. As can be seen in Table II, the geometrical parameters are only slightly changed by the use of the new functional with a concomitantly small variation in the adsorption energy that decreases by 2 to 32.1 kcal/mol .

A comparison of the results from the present work with previous theoretical calculations is provided in Table II. The most recent results were based on a DFT cluster model and FLAPW slab calculations by NNBB. As can be seen from these data, the geometrical parameters obtained in the current study compare quite well with the more expensive FLAPW results based on the Perdew, Burke, and Ernzerhof (PBE) functional.³⁰ A similarly good agreement is found between our geometrical parameters and their parameters computed from atomic orbital-based cluster calculations determined with the PW91 functional. NNBB calculated the adsorption energies based exclusively on the use of a 22 atom iron cluster, and obtained an adsorption energy of 32.3 kcal/mol in the case of the on-top configuration. This value is very close to our energies of 34.1 or 32.1 kcal/mol for $\theta = 0.25$ using the PW91 or the revPBE functionals, respectively.

Focusing now on the experimental data for binding energies (see Table II), we observe some large variations among various studies. Moon *et al.*⁶ have determined from TPD data based on first-order desorption kinetics an activation energy for desorption from the on-top position of 12.8 kcal/mol . This value differs significantly with the theoretical results obtained from both the current study and NNBB. Even if we allow for the possibility of adjustments to larger pre-exponentials^{6b} as presented in the Introduction, the experimental value would still be only $16\text{--}18 \text{ kcal/mol}$. Given these differences we believe that further experimental work would be highly desirable to firmly establish the adsorption energy of CO at the onefold site on the Fe(100) surface.

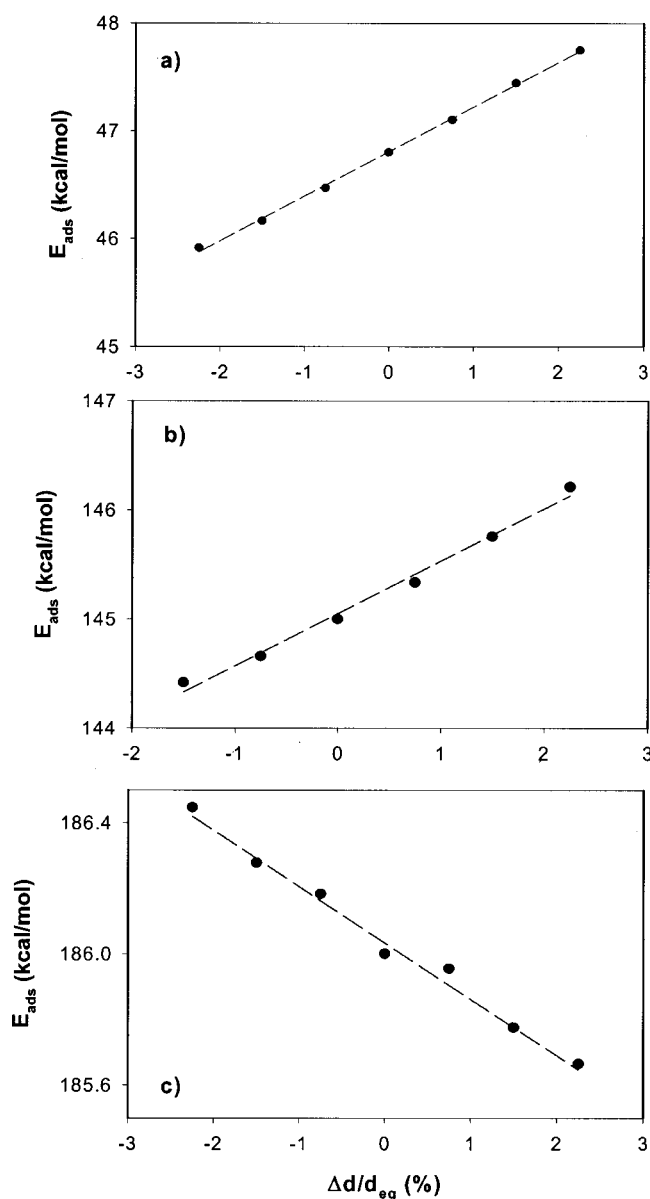


FIG. 3. Variations of the adsorption energies for (a) CO, (b) O, and (c) C species adsorbed at the fourfold hollow site as a function of the relative change in the surface lattice constant $(d - d_{eq})/d_{eq}$ of the Fe(100) surface (see Sec. III F for further details). Dashed lines are drawn as a guide to the eye.

A problem of interest in previous experimental studies was the attempt to associate the binding site with the spectral shifts in the C-O stretching frequency as the CO molecule adsorbs at various sites on the Fe(100) surface. Moon *et al.*^{7,9} have assigned, based on high resolution electron energy loss spectroscopy (HREELS), a C-O vibrational frequency of 2070 cm^{-1} for the on-top adsorption configuration. This corresponds to a redshift of about 73 cm^{-1} relative to the experimental gas phase frequency.³⁷ In our studies we have determined the CO stretching frequency adsorbed in the on-top configuration. In this calculation the C and O atoms were moved such that the center of mass of the CO molecule is held fixed. The minimum potential energy value corresponds to that determined after relaxation of the slab-CO system.

The vibrational frequency has then been obtained from a polynomial interpolation of the variation of total energy with the interatomic C-O distance. Based on this procedure we have determined a CO stretching frequency of 1887 cm^{-1} . This is consistent with the experimental finding of a redshift from the gas phase, but the magnitude of the theoretical shift is significantly larger at 287 cm^{-1} than the experimentally observed shift. It is interesting to note that NNBB obtained a value of 1888 cm^{-1} for the case of a CO molecule adsorbed on a single Fe atom, in remarkable agreement with the value determined from the current slab model calculations. The similarity between the two sets of calculated values supports the previous findings¹⁸ that the bonding in this state is quite local. The absolute difference between the theoretical and experimental stretching frequencies at the onefold site is 183 cm^{-1} . Discussions concerning possible causes for this difference in frequencies will be deferred to the section covering CO bound at the twofold site.

Twofold (bridged) site. The twofold site corresponds to a bridged configuration with CO adsorbed between two nearest-neighbor surface Fe ions. In this case we have determined two different geometries [see Figs. 1(b) and 1(c)] corresponding to two stationary points on the potential surface. The geometrical parameters for the bridged configurations are indicated in Table II. In the first case, the CO molecule is tilted relative to the surface normal while in the second case it remains perpendicular to the surface. For these two geometries the CO bond lengths are similar, i.e., elongated by 0.048 and 0.051 \AA relative to the isolated gas phase equilibrium distance. At $\theta=0.25$ coverage, the tilted configuration has an adsorption energy of 34.8 kcal/mol , which is slightly larger than the 32.9 kcal/mol found for the vertical orientation. This order of stability is maintained even at the higher coverage of $\theta=0.5$, where CO molecules are placed in a next-nearest-neighbors configuration, producing a decrease in adsorption energies to 30.9 and 26.0 kcal/mol for the tilted and vertical configurations, respectively. Additionally, tests have been run to check the relationship between the adsorption energy and the number of layers in the slab model. As indicated in Table II, the calculated geometric and energetic parameters for the bridged configurations are practically unchanged going from a six-layer slab to a seven-layer slab, justifying the use of the six-layer slab in the remaining calculations.

However, we have determined that the adsorption energy shows a small dependence of about $2\text{--}3 \text{ kcal/mol}$ between the two exchange-correlation functionals used here. Indeed, similar to the case of the on-top configuration, the use of the revPBE functional decreases slightly the adsorption energies at $\theta=0.25$ to 32.3 and 29.7 kcal/mol for the tilted and vertical configurations, respectively. These energetic variations take place without any significant changes to the CO bond length or its orientation relative to the surface.

Comparisons will now be made between the current results in Table II and those obtained by NNBB based on FLAPW calculations. It should be noted that these authors have considered only the vertical bridged configuration thereby restricting the comparison to only this structure. In this case the agreement between the two sets of values is

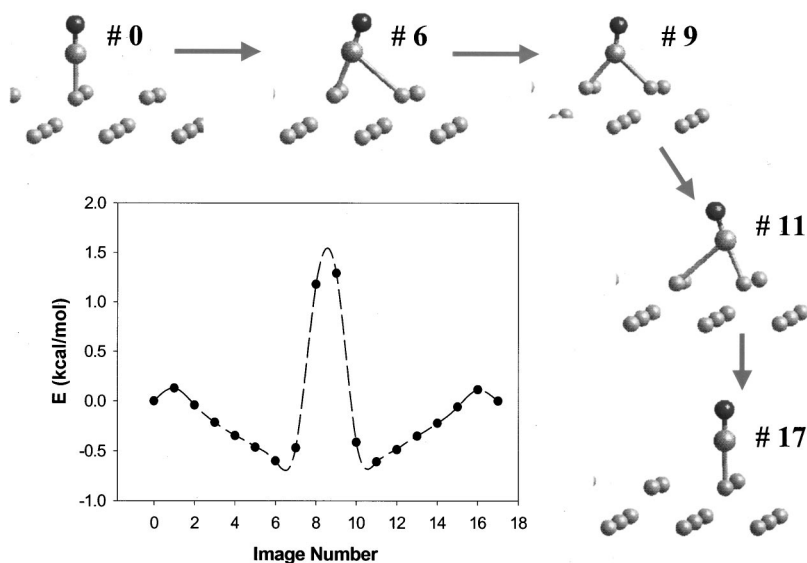


FIG. 4. Potential energy surface for diffusion of a CO molecule from a onefold site to the neighboring onefold site. The chosen path is through a twofold tilted configuration. Each chemical structure is labeled with its nudged elastic band image number corresponding to the “image number” in the potential energy plot. This holds for images in Fig. 4–8.

very good. For example, our predicted C-O and Fe-C distances are 1.196 and 1.957 Å, respectively, while the FLAPW results are 1.18 and 1.95 Å. However, both sets of values differ more significantly from the results in cluster calculations. For example, in the case of Fe-C distances, differences as large as 0.16 Å exist. As noted by NNBB, such differences are in part related to the limitations of the cluster model and might be due also to an insufficient relaxation of the Fe atoms in the cluster.

In addition to these geometric variations, one can see larger differences for the adsorption energies between our values and those determined in NNBB’s cluster calculations.¹⁸ For example, in the vertical bridged configuration at $\theta=0.25$, the binding energies are 29.7 or 32.9 kcal/mol depending on the choice of functional. NNBB have determined a value of 24.7 kcal/mol. Despite these differences of about 5–8 kcal/mol, both sets of calculated results support the fact that the binding energy for the twofold vertical configuration is smaller than for the on-top site. This conclusion is opposite to what was reported from experiment^{6a} where it

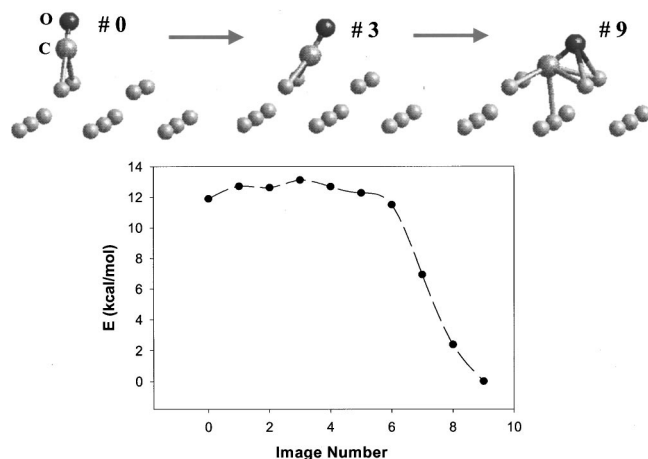


FIG. 5. Potential energy surface for diffusion of a CO molecule from a two-fold tilted configuration to a neighboring fourfold hollow site.

was assumed that the bridged vertical configuration has a binding energy of 18.0 kcal/mol, and consequently this state is more strongly bound than the on-top configuration at 12.8 kcal/mol. Our results suggest that the 18 kcal/mol experimental desorption energy corresponds more likely to a tilted bridged configuration or the on-top structure, but not the bridged vertical configuration.

Based on the frozen-phonon approach, the vibrational frequency for the C-O stretch in the twofold tilted configuration is calculated to be 1784 cm^{-1} (see Table II). This is a redshift of 103 cm^{-1} relative to the on-top vibrational frequency. A similar redshift has been determined by NNBB for the twofold configuration relative to the onefold configuration. However, their calculated shift is much larger, namely, 195 cm^{-1} , and corresponds to the vertical (rather than the tilted) twofold configuration. The value of the vibrational frequency of CO in the α_2 state has been the subject of various experimental studies. In two such studies,^{7,9} the band at 2020 cm^{-1} was assigned to the CO stretch at the α_2 (twofold) site. The experimental shift in the frequency from the onefold to the twofold sites is a redshift of 50 cm^{-1} . Theory also predicts a redshift going from the α_1 to the α_2 sites, but the magnitude of the shift is twice as large at 103 cm^{-1} .

Fourfold configuration. The third important adsorption configuration we have analyzed is at the fourfold hollow site. As can be seen from Fig. 1(d), the molecule is oriented along $\langle 100 \rangle$ azimuths with the C atom down and tilted by 50° with respect to a normal to the surface. This geometry allows for simultaneous interaction of both C and O atoms with Fe surface atoms. As a result there is an increase of the binding energy to 46.7 kcal/mol (see Table II), which is significantly larger than those corresponding to the on-top or bridged configurations.

For the sake of completeness, a fourfold vertical structure has been sought and located, and its characteristics are given in Table II. A NEB calculation predicts this vertical geometry to be an energy maximum along a path that connects the two minimum energy structures at the 50° tilt angle (i.e., CO tilted towards either side of the fourfold site and equivalent

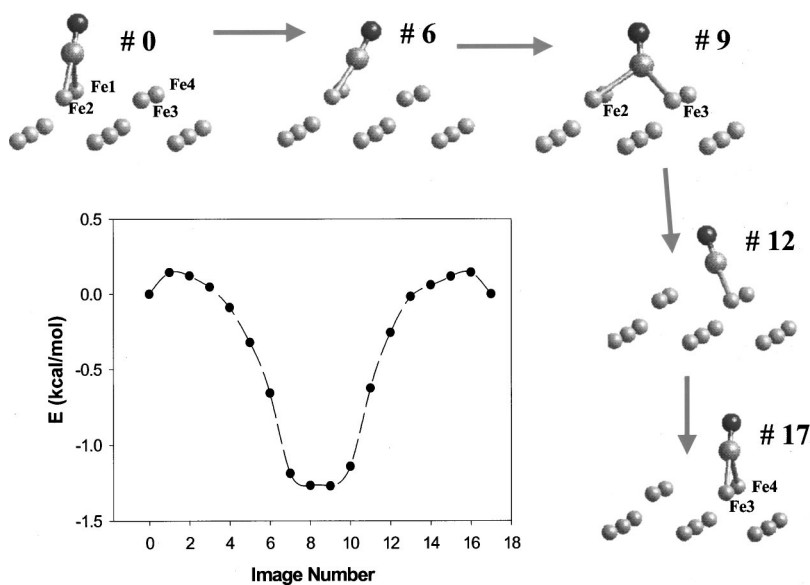


FIG. 6. Potential energy surface for motion of a CO molecule starting from a twofold tilted configuration between Fe1-Fe2 atoms and ending in a twofold tilted configuration between Fe3-Fe4. The path involves bonding to the Fe2-Fe3 atoms with a tilt of CO bond toward the fourfold hollow site.

by symmetry). The CO bond length has decreased to 1.26 Å, and the adsorption energy has decreased by about 10 kcal/mol relative to the tilted configuration. The trends in these two properties suggest that the oxygen is bonding to the iron in the tilted configuration but not in the vertical geometry.

The existence of an “unusual” elongated CO bond seen in experimental investigations⁸ is substantiated by our calculations. We find that the C-O bond is elongated by 0.17 Å relative to the isolated gas-phase molecule or by 0.13–0.15 Å relative to the bond length of CO in α_2 and α_1 states. NEXAFS measurements⁸ on the fourfold configuration have determined an elongation by 0.07 ± 0.02 Å of the CO bond relative to either the bridged or on-top states. Our results overestimate slightly this value but they are practically identical to those obtained by NNBB based on PW91 cluster calculations (see data in Table II). The tilt angle determined in our study is also only 4° smaller than the one predicted by NNBB (see Table II) and agrees very well with the experimental results that indicate a tilt angle between $45^\circ \pm 10^\circ$ (Ref. 9) and $55^\circ \pm 2^\circ$.¹⁰

We have also analyzed how the adsorption energies and

the geometrical parameters of this fourfold state depend on the thickness of the slab used in calculations. As indicated in Table II, the increase from six to seven Fe layers does not produce any appreciable change in either geometries or adsorption energies. However, as seen in the case of the onefold and twofold sites, the use of the revPBE functional again decreases the adsorption energy by about 3 to 43.8 kcal/mol. The corresponding binding energy determined by NNBB of 37.4 kcal/mol is smaller than the aforementioned value, but in their case only the five Fe atoms of the cluster bonded directly to the C atom were allowed to relax. As they mention in their article,¹⁸ further surface relaxations could increase the binding energies, thereby decreasing the gap between the two calculated values. All the calculated binding energies for the fourfold state are larger than the corresponding experimental value of 26.2 kcal/mol,⁶ (or 32–36 kcal/mol for the adjusted pre-exponential) analogous to what was seen for the onefold and twofold cases.

The stretching vibrational frequency we have calculated for the CO molecule adsorbed at the fourfold hollow site is 1246 cm^{-1} . This value represents an extremely low

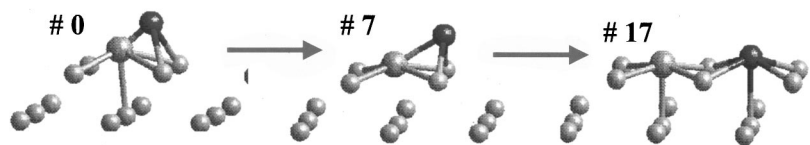
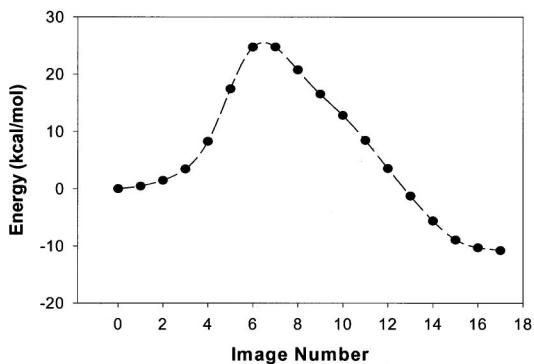


FIG. 7. Potential energy surface for dissociation of a CO molecule at the fourfold hollow site. The final configuration corresponds to C and O atoms adsorbed at two different, but nearest-neighbor fourfold hollow sites.

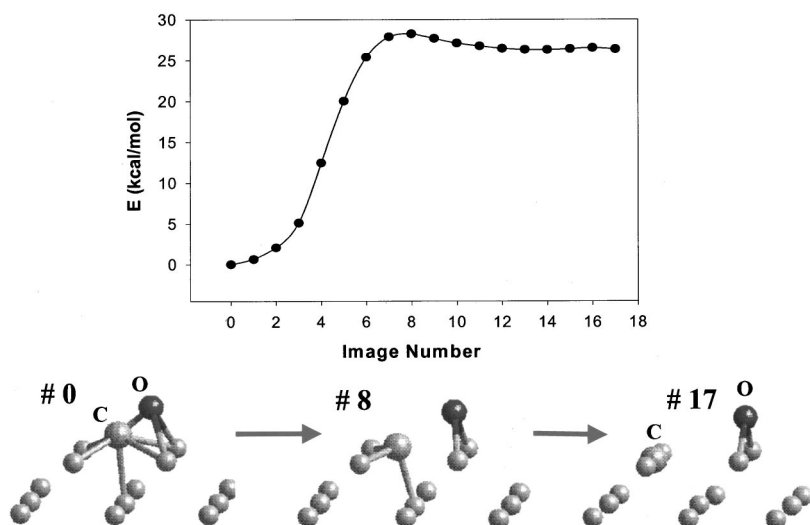


FIG. 8. Potential energy surface for dissociation of a CO molecule at the fourfold hollow site. The final configuration corresponds to C and O atoms adsorbed at two opposite twofold sites.

vibrational frequency when compared with the gas phase value, and confirms the experimental findings that indicate a vibrational frequency for this state in the range of 1135–1260 cm^{-1} depending upon temperature and surface coverage.^{7,8,9,10,12,13}

Finally, for the sake of completeness, it is worth mentioning one experimental heat of adsorption reported in 1978 by Welder *et al.*³⁹ based on “calorimetric adsorption heats.” Their experiment used a polycrystalline thin film of iron, so direct comparison with results on a bcc (100) surface is not possible. However, at 273 K they recorded the heat of adsorption for CO as a function of surface coverage, and reported a curve with three steps or “regions.” In the lowest coverage region the heat of adsorption is reported to be 37.0 kcal/mol, in fairly good agreement with the theoretical results for adsorption at the α_3 site. Unfortunately, because the surface is polycrystalline, one can not say *a priori* that the sites being occupied at the lowest coverage in their experiment are indeed the α_3 sites.

E. Adsorption of C and O atoms on the Fe(100) surface

In addition to the CO molecular adsorption, we have studied the adsorption of individual C and O atoms on Fe(100). A pictorial view of the resulting equilibrium configurations are given in Fig. 2, and the corresponding geometric and energetic parameters are detailed in Table III. Similar to the CO adsorption, the most stable configuration for the C atom is in the fourfold hollow site. In this case the adsorption energy is quite large with a value of 186 kcal/mol. For the three adsorption configurations, i.e., fourfold (4f), twofold (2f), and onefold (1f), the order of stability is calculated unambiguously as $E(4f) > E(2f) > E(1f)$. An interesting adsorption geometry is determined for the case of the twofold bridged configuration where the C atom embeds into the lattice [Fig. 2(b)]. In this position, the C atom is only 0.127 Å above the Fe surface plane in an almost linear configuration with the neighboring Fe atoms forming a Fe-C-Fe angle of 171.5°. For the O atom we find a similar stability ranking $E(4f) > E(2f) > E(1f)$ with a maximum adsorption energy at the fourfold site of 145 kcal/mol, which is 41 kcal/mol less

stable than the carbon analog. At the twofold site the O atom remains well above the Fe surface at about 1.241 Å unlike the C atom that embeds into the lattice.

F. Strain effects on molecular and atomic adsorption

In practical applications there are many instances when the Fe surface is strained instead of relaxed. Examples include the case of various local deformations of a single metal phase or in the case of bimetallic overlayers.^{40,41} Consequently, it becomes important to investigate how the chemisorption properties of molecular and atomic species change on such strained surfaces. This problem has been investigated theoretically by Mavrikakis *et al.*⁴² for the case of CO adsorption on the Ru(0001) surface where it was found that a strong correlation exists between the surface strain and the adsorption energies. It was shown that these effects could be attributed to an up-shift of the center of the metal *d* bands with strain. Such results have important consequences as the surface strain can be used to further modify the catalytic activity of the metallic surfaces.

In the present study, the lattice strain is induced by simultaneously changing those two lattice constants that are parallel to the surface for the Fe(100) slab. These changes amount to maximum variations of approximately $\pm 2\%$ relative to the equilibrium structure of the lattice parameters ($d_{\text{eq}} = 2.8653$ Å). In all these calculations the distance between the surface layers is kept fixed at the value determined for the relaxed, unstrained layers. The calculations have been done for the case of the CO molecule as well as for the individual O and C atoms adsorbed at the fourfold hollow site.

The corresponding variations of the adsorption energies are illustrated in Fig. 3. As can be seen, there is a significant variation of the adsorption energies with the amount of surface stress, particularly for the CO and O species. For both these cases the chemisorption energies increase by almost 2 kcal/mol with lattice expansion [see Figs. 3(a) and 3(b)]. This effect is similar to the one found previously for the case of CO and O on Ru(0001).⁴² For the case of the C atom, we find a reversed effect, i.e., the adsorption energy decreases

with lattice expansion. However, in this case the variation of the C adsorption energy with the amount of lattice strain is smaller than the one found for the O atom, with the energy decreasing by only about 1 kcal/mol over this range of lattice changes.

G. Minimum energy paths for diffusion of a CO molecule on the Fe(100) surface

Three minimum energy paths are calculated to describe the motion of the CO molecule between various equilibrium sites. The first one corresponds to the motion between two onefold adsorption configurations, the second connects the twofold tilted configuration with the fourfold state, and the third corresponds to the motion between two twofold configurations along a path that involves atoms Fe2→Fe3→Fe4 (see Fig. 6). The minimum energy paths corresponding to these processes are represented in Figs. 4–6.

In the case of motion between two onefold sites, it can be seen in Fig. 4 that the potential surface has two local minima in the region close to images 6 and 11. These configurations correspond to the tilted twofold (bridged) states described previously. Between these configurations there is a barrier of about 2 kcal/mol. The molecular configuration corresponding to the top of the barrier is the bridged vertical structure, leading one to the conclusion that the vertical twofold configuration is a transition state and not a local minimum. Due to the limited number of images used in this calculation, it is possible that a very small local minimum might exist at the top of the potential profile given in Fig. 4. However, such a minimum would be of little practical importance. This potential energy profile shows that the onefold configuration (images 0 and 17 in Fig. 4) is energetically only slightly less favorable than the tilted twofold configuration (images 6 and 11), and both these two states are more stable than the vertical twofold configuration, as previously discussed.

The PES describing the motion from the twofold tilted state to the fourfold configuration (see Fig. 5) indicates that the potential energy curve is initially quite flat, rising by only 1 kcal/mol for the first five images, followed by a pronounced decrease as the CO enters the hollow site. It is clear that once a CO molecule is adsorbed at the twofold site it will diffuse easily to a fourfold configuration even at low temperature.

Finally, we have analyzed a diffusion path from a twofold tilted configuration to another twofold tilted configuration that takes place along a path involving the iron atoms Fe2, Fe3, and Fe4 (see Fig. 6). The CO molecule starts from a bridged configuration between the Fe1 and Fe2 atoms, followed by binding between Fe2 and Fe3 and finally reaching the bridged twofold tilted state between Fe3 and Fe4. As in the previous cases, the activation energies for this diffusion path are small, with the barrier for motion from the bridged tilted configuration to the configuration between Fe2-Fe3 atoms being only 0.14 kcal/mol, while the central minimum is separated by neighboring minima with barriers of 1.4 kcal/mol.

The above results indicate that the diffusion barriers between the onefold→twofold configurations, as well as be-

tween the twofold→fourfold configurations are quite small with values below 1.8 kcal/mol. In contrast, diffusion out of the fourfold configuration requires significantly more energy, as demonstrated for diffusion into the twofold site where the barrier is 13.1 kcal/mol. These findings indicate that even in the low-temperature regime, CO molecules can diffuse easily among different adsorption sites until they reach the fourfold sites. Once CO gets to the fourfold site, the diffusion out again is more difficult due to the higher barriers. This result is consistent with experimental data^{6a,9} that indicate the α_3 (fourfold) state is the first to be filled as a function of increasing exposure to CO gas.

H. Minimum energy paths for CO dissociation on the Fe(100) surface

As indicated by previous experimental studies⁷ the dissociation of a CO molecule takes place starting from the α_3 state corresponding to the fourfold configuration. In this state, the C-O bond is elongated and weakened as indicated by the very low vibrational frequency. The other two molecular states, i.e., CO(α_2) and CO(α_1), desorb molecularly without dissociation. Consequently, in this study we focus exclusively on the investigation of the PES corresponding to dissociation of a CO molecule starting from a fourfold adsorption configuration.

For this purpose, two important reaction paths have been analyzed. The first one corresponds to the case when the C atom remains localized in the same potential well as the CO molecule and only the O atom migrates to a neighboring fourfold site. The second process corresponds to a concerted mechanism in which both C and O atoms move away from the initial site and end up in twofold configurations on opposite sides of the initial hollow site. The profiles for these reactions are depicted in Figs. 7 and 8, respectively. As can be seen in these figures, the barrier heights for both of these processes are comparable to one another, with values of 24.5 and 28.2 kcal/mol, respectively. In the case of the second reaction path it is possible that C and O atoms will continue to move away from each other such that they will end up in fourfold minima separated by an unoccupied hollow site, or an intermediate such as carbon in the twofold and oxygen proceeding to the fourfold site. We have not investigated these cases, as they require a slab model employing a larger supercell than the one considered in the present calculations.

It is important to note that the activation energies determined in this study are significantly smaller than those reported previously by Blyholder and Lawless (BL).¹⁶ Based on MINDO/SR calculations they determined activation energies for multiple dissociation pathways of CO on a 12 atom iron cluster. The two paths most closely corresponding to our paths start with CO in a fourfold configuration. In the first case, C remains in the initial fourfold site while O moves into a neighboring fourfold site. For this reaction they calculate a barrier of ~ 100 kcal/mol. This barrier should be compared to the current barrier of 24.5 kcal/mol for a similar reaction path given in Fig. 7. BL's second case corresponds to a path in which both C and O atoms end in twofold sites. This process was found to have the lowest dissociation bar-

rier of 65 kcal/mol among those investigated by these authors. This pathway is analogous to the one shown in Fig. 8, which has a barrier to dissociation of only 28.2 kcal/mol. It is worth noting that BL's values for dissociation are significantly larger than the experimental and most recent theoretical predictions for the adsorption energy of CO in the α_3 state. In contrast, our values for the activation energy of the CO dissociation are approximately equal to the experimental adsorption energy at the fourfold site, and below the theoretical predictions from BL. The current results, unlike BL's, support the model proposed by Cameron and Dwyer¹¹ in which, for temperatures above 440 K, the dissociation process precludes or competes with the desorption process.

IV. CONCLUSION

Based on a periodic slab model, we have identified the existence of three adsorption configurations for CO on the surface. The order of stability for these configurations is $E(4f) > E(2f, \text{tilt}) \approx E(1f)$ at lower coverages, and $E(4f) > E(1f) > E(2f, \text{tilt})$ at higher coverages. It is worth noting that the difference in adsorption energy between the $E(1f)$ and $E(2f, \text{tilt})$ is only 2.5 kcal/mol at this higher coverage. The bridged tilted (twofold) configuration we propose in this study has not been considered previously in either theoretical or experimental investigations. Our results suggest that both the onefold and tilted twofold configurations are more stable than the twofold vertical configuration by about 1–2 kcal/mol at a coverage of $\theta = 0.25$, and about 5–7 kcal/mol at $\theta = 0.5$ coverage. The most stable adsorption configuration is the fourfold state in which the CO molecule is tilted by about 50° relative to the surface normal. In this configuration the C-O bond is stretched by 0.13–0.15 Å relative to the onefold or twofold configurations. Additionally the CO vibrational frequency of 1246 cm^{-1} in this state is significantly smaller than for isolated CO, in agreement with previous experimental findings.⁸

Calculations of the adsorption energies for isolated C and O atoms predicts the order of stability to be $E(4f) > E(2f) > E(1f)$, with C bonding more strongly at each site than O.

Another major difference between the two atomic species is found in the case of the twofold configuration in which the O atom adsorbs above the surface plane while the C atom embeds into the Fe surface. Finally, at each site the C or O atom binds more strongly than molecular CO by at least a factor of 3.

Potential energy surfaces for surface diffusion of CO between equilibrium configurations indicate several important features. First, the twofold vertical configuration corresponds to an apparent transition state rather than a minimum as was considered previously.^{8,18} Second, the barriers for diffusion away from the onefold sites or twofold sites are small, with values below 1.8 kcal/mol. Third, the diffusion barrier out of the fourfold site is significantly larger with a value of at least 13.1 kcal/mol. These data support the experimental finding that the CO molecule will first fill the fourfold hollow sites at lower temperatures.

Starting from a fourfold configuration, two possible paths for decomposition of CO have been analyzed on the Fe(100). The first one corresponds to a sequential mechanism in which the CO bond is stretched continuously but the C atom remains at the original fourfold site. The second path is a concerted mechanism in which both C and O atoms are moving away from each other and from the original fourfold site. The activation barriers for these two processes have been found equal to 24.5 and 28.2 kcal/mol, respectively. These values are smaller than the corresponding adsorption energy at the fourfold site, and support the experimental finding^{6a} at 440 K that indicates dissociation from a fourfold site precludes or competes with the molecular desorption.

ACKNOWLEDGMENTS

We gratefully acknowledge the computational resources provided under a Challenge award received from the DOD High Performance Computing Modernization Office, and by ARL MSRC supercomputer center. D.L.T. gratefully acknowledges partial support from the Army Research Laboratory.

¹J. T. Yates, Jr., T. E. Madey, and J. C. Campuzano, in *The Chemical Physics of Solid Surfaces and Heterogeneous Catalysis* edited by D. A. King and D. P. Woodruff (Elsevier, Amsterdam, 1990), Vol. 3.

²G. A. Somorjai, *Introduction to Surface Chemistry and Catalysis* (Wiley, New York, 1994).

³(a) F. Fischer and H. Tropsch, *Brennst. Chem.* **4**, 276 (1923); (b) R. B. Anderson, *The Fischer-Tropsch Synthesis* (Academic, Orlando, FL, 1984).

⁴W. N. Delagass (unpublished).

⁵(a) J. T. Yates, Jr., *Surf. Sci.* **299**, 731 (1994). (b) J. C. Campuzano, *The Chemical Physics of Solid Surfaces and Heterogeneous Catalysis* (Ref. 1).

⁶(a) D. W. Moon, D. J. Dwyer, and S. L. Bernasek, *Surf. Sci.* **163**, 215 (1985); (b) L. J. Whitman, L. J. Richter, B. A. Gurney, J. S.

Villarubia, and W. Ho, *J. Chem. Phys.* **90**, 2050 (1989).

⁷D. W. Moon, S. L. Bernasek, J. P. Lu, J. L. Gland, and D. J. Dwyer, *Surf. Sci.* **184**, 90 (1987).

⁸D. W. Moon, S. Cameron, F. Zaera, W. Eberhardt, R. Carr, S. L. Bernasek, J. L. Gland, and D. J. Dwyer, *Surf. Sci.* **180**, L123 (1987).

⁹D. W. Moon, S. L. Bernasek, D. J. Dwyer, and J. L. Gland, *J. Am. Chem. Soc.* **107**, 4363 (1985).

¹⁰R. S. Saiki, G. S. Herman, M. Yamada, J. Osterwalder, and C. S. Fadley, *Phys. Rev. Lett.* **17**, 283 (1989).

¹¹S. D. Cameron and D. J. Dwyer, *Langmuir* **4**, 282 (1988).

¹²J. P. Lu, M. R. Albert, and S. L. Bernasek, *Surf. Sci.* **217**, 55 (1989).

¹³S. L. Bernasek, *Annu. Rev. Phys. Chem.* **44**, 265 (1993).

¹⁴S. P. Mehandru and A. B. Anderson, *Surf. Sci.* **201**, 345 (1988).

- ¹⁵T. E. Meehan and J. D. Head, Surf. Sci. Lett. **243**, L55 (1991).
- ¹⁶G. Blyholder and M. Lawless, Surf. Sci. **290**, 155 (1993).
- ¹⁷Y. Aray and J. Rodrigues, Surf. Sci. **405**, L532 (1998).
- ¹⁸S. K. Nayak, M. Nooijen, S. L. Bernasek, and P. Blaha, J. Phys. Chem. B **105**, 164 (2001).
- ¹⁹G. Kresse and J. Hafner, Phys. Rev. B **47**, 558 (1993); **49**, 14 251 (1994).
- ²⁰G. Kresse and J. Furthmüller, Comput. Mater. Sci. **6**, 15 (1996).
- ²¹G. Kresse and J. Furthmüller, Phys. Rev. B **54**, 11 169 (1996).
- ²²D. Vanderbilt, Phys. Rev. B **41**, 7892 (1990).
- ²³G. Kresse and J. Hafner, J. Phys.: Condens. Matter **6**, 8245 (1994).
- ²⁴E. G. Moroni, G. Kresse, J. Hafner, and J. Furthmüller, Phys. Rev. B **56**, 15 629 (1997).
- ²⁵H. J. Monkhorst and J. D. Pack, Phys. Rev. B **13**, 5188 (1976).
- ²⁶M. Methfessel and A. T. Paxton, Phys. Rev. B **40**, 3616 (1989).
- ²⁷G. Kresse and J. Hafner, Phys. Rev. B **47**, 558 (1993).
- ²⁸(a) G. Mills and H. Jónsson, Phys. Rev. Lett. **72**, 1124 (1994); (b) G. Mills, H. Jónsson, and G. K. Schenter, Surf. Sci. **324**, 305 (1995); (c) H. Jónsson, G. Mills, and K. W. Jacobsen, in *Classical Quantum Dynamics in Condensed Phase Simulations*, edited by B. J. Berne, G. Ciccotti, and D. F. Coker (World Scientific, Singapore, 1998), p. 385.
- ²⁹(a) J. P. Perdew and Y. Wang, Phys. Rev. B **45**, 13 244 (1992). (b) J. P. Perdew, J. A. Chevary, S. H. Vosko, K. A. Jackson, M. R. Pedersen, D. J. Singh, and C. Frolhais, *ibid.* **46**, 6671 (1992).
- ³⁰J. P. Perdew, K. Burke, and M. Ernzerhof, Phys. Rev. Lett. **77**, 3865 (1996).
- ³¹B. Hammer, L. B. Hansen, and J. K. Nørskov, Phys. Rev. B **59**, 7413 (1999).
- ³²V. Milman, B. Winkler, J. A. White, C. J. Pickard, M. C. Payne, E. V. Akhmatkaya, and R. H. Nobes, Int. J. Quantum Chem. **77**, 895 (2000).
- ³³F. D. Murnaghan, Proc. Natl. Acad. Sci. U.S.A. **30**, 2344 (1944).
- ³⁴C. Kittel, *Introduction to Solid State Physics* (Wiley, New York, 1996).
- ³⁵J. J. Mortensen, M. V. Ganduglia-Pirovano, L. B. Hansen, B. Hammer, P. Stoltze, and J. K. Nørskov, Surf. Sci. **8**, 422 (1999).
- ³⁶Z. Q. Wang, Y. S. Li, F. Jona, and P. M. Marcus, Solid State Commun. **61**, 623 (1987).
- ³⁷K. P. Huber and G. Herzberg, *Molecular Spectra and Molecular Structure VI. Constants of Diatomic Molecules* (Van Nostrand, Reinhold, 1979).
- ³⁸Y. Zhang and W. Yang, Phys. Rev. Lett. **80**, 890 (1998).
- ³⁹G. Welder, K. G. Colb, G. McElhiney, and W. Heinrich, Appl. Surf. Sci. **2**, 30 (1978).
- ⁴⁰M. Gsell, P. Jakob, and D. Menzel, Science **280**, 717 (1998).
- ⁴¹J. H. Larsen and I. Chorkendorff, Surf. Sci. **405**, 62 (1998).
- ⁴²M. Mavrikakis, B. Hammer, and J. K. Nørskov, Phys. Rev. Lett. **81**, 2819 (1998).